Nonlinear time history analysis of a pre-stressed concrete containment vessel model under Japan's March 11 earthquake

An Duan[1], Zuo-zhou Zhao[*2], Ju Chen[1], Jia-ru Qian[2] and Wei-liang Jin[1]

[1]*College of Civil Engineering and Architecture, Zhejiang University, Hangzhou 310058, China*
[2]*Key Laboratory of Civil Engineering Safety and Durability of China Education Ministry, Tsinghua University, Beijing 100084, China*

Abstract. To evaluate the behavior of the advanced unbonded pre-stressed concrete containment vessel (UPCCV) for one typical China nuclear power plant under Japan's March 11 earthquake, five nonlinear time history analysis and a nonlinear static analysis of a 1:10 scale UPCCV structure have been carried out with MSC.MARC finite element program. Comparisons between the analytical and experimental results demonstrated that the developed finite element model can predict the earthquake behavior of the UPCCV with fair accuracy. The responses of the 1:10 scale UPCCV subjected to the 11 March 2011 Japan earthquakes recorded at the MYG003 station with the peak ground acceleration (PGA) of 781 gal and at the MYG013 station with the PGA of 982 gal were predicted by the dynamic analysis. Finally, a static analysis was performed to seek the ultimate load carrying capacity for the 1:10 scale UPCCV.

1. Introduction

As the ultimate barrier against the release of radioactivity, the concrete containment vessel is a very important structure of nuclear power plant. In 2006, an advanced unbonded pre-stressed concrete containment vessel (UPCCV) for one typical China nuclear power plant was designed by Shanghai Nuclear Engineering Research & Design Institute. Since the UPCCV is required to resist earthquakes, a pseudo-dynamic test of a 1/10 scale UPCCV model structure has been conducted at Tsinghua University, Beijing China in 2006 (Qian *et al.* 2007). The test results and a push over analysis (Duan and Qian 2009) show that the advanced UPCCV would remain elastic under the safe shutdown earthquake (SSE) of the US criteria.

On March 11, 2011, a devastating earthquake and tsunami hit Japan, and the Fukushima Daiichi 1 nuclear reactor plant was destroyed. This earthquake raised again profound concern regarding the seismic performance of the nuclear power plants around the world.

In fact, during the past years a large number of experimental and analytical studies focused on

---

*Corresponding author, Associate Professor, E-mail: zzzhao@mail.tsinghua.edu.cn

the seismic capacity of containment vessel. In Japan, the Nuclear Power Engineering Corporation has conducted a series of shaking table tests on a 1/8 scale concrete containment vessel model to validate its seismic design and reliability under destructive earthquakes (Hirama *et al*. 2005a, b). Lee and Song (1999) used a seismic fragility method and a conservative deterministic failure margin method to evaluate the seismic safety for the containment structure of the Yonggwang Nuclear Power Plant. In recent years, numerical simulation has become popular with the rapid development of computer technology. Many studies have been made on the simulations of the behavior of the nuclear containment under pressure loading far beyond the design basis by using finite element method (Bash *et al*. 2003, Prinja *et al*. 2005). However, researches on the nonlinear time history analysis of the containment vessel subjected to earthquakes are limited (Kobayashi *et al*. 2002, Frano *et al*. 2010). The nonlinear time history analysis is the most sophisticated and powerful method in earthquake engineering assessment. It can calculate the displacements, stresses, strains, damaged positions at any time during the earthquake excitation for the structure. Frano *et al*. (2010) carried out a time history analysis for the IRIS containment under an earthquake excitation with the peak ground acceleration (PGA) of 0.3g, and the acceleration and displacement time histories were predicted. The PGA of the Japan's March 11 earthquake is much larger than 0.3g. Moreover, the detailed responses (like stress and strain distributions, cracking positions) of the advanced UPCCV subjected to this strong earthquake are demanded.

Hence, this paper presents a nonlinear 3-D dynamic time history analysis carried out with MSC.MARC finite element (FE) program (MSC 2007a) to predict the global and local response of the advanced UPCCV for one typical China nuclear power plant under Japan's March 11 earthquake.

2. The UPCCV test model

Due to loading limitations, the pseudo-dynamic test model had to be geometrically reduced from the original prototype. Hence, a 1:10 scale model structure of the advanced UPCCV for one typical China nuclear power plant was constructed. An overall geometry and a photo of the test model are shown in Fig. 1. The test structure represented all the main structural features of the advanced UPCCV which is an unbonded pre-stressed concrete cylinder with a hemispherical dome, two vertical buttresses and a base mat.

(a) Photo of the test model
Fig. 1 Photo and geometry of the test UPCCV model structure
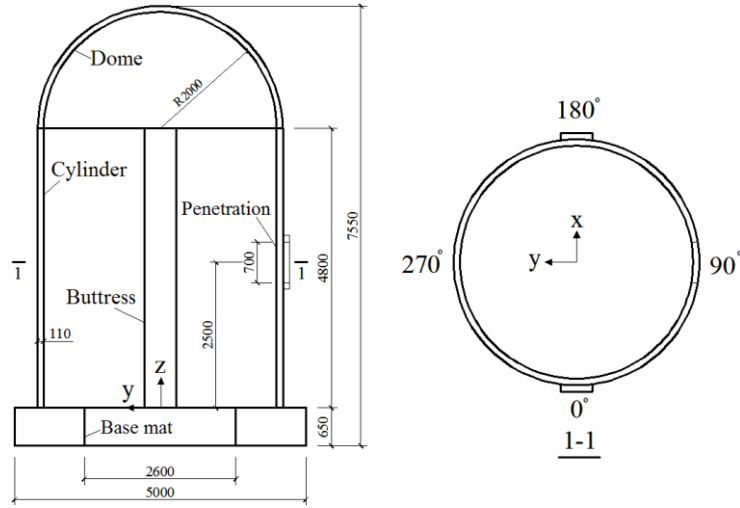
(b) Geometry of the test model

Fig. 1 Continued

3. Mathematical modelling

Predicting response of a complex structure like a UPCCV under a strong earthquake needs complicated nonlinear analysis. The nonlinear analysis was carried out on the 1:10 scale UPCCV test structure by using MSC.MARC FE program. Examples and benchmarks (Lu *et al*. 2007, Li *et al*. 2011, Miao *et al*. 2011, Lu *et al*. 2012) show that this program can precisely simulate the nonlinear behaviours of reinforced concrete structures. Fig. 2 presents the 3D FE model.

3.1 Modelling of the structural features

The cylinder and the dome were modeled with 4-node, thin shell elements (Elements 139). The integration through the shell thickness was performed numerically using Simpson's rule (MSC 2007b), and seven integration points were specified. The base mat was modeled with 8-node, isoparametric, arbitrary hexahedral solid elements (Elements 7). The buttresses were modeled with beam elements (Elements 98). The reinforcements were modeled with 4-node, isoparametric, quadrilateral membrane elements (Elements 18) which was inserted into the shell elements, assuming a perfect bonding between the steel bars and the surrounding concrete. The vertical and hoop tendons in the cylinder were modeled explicitly with 2-node, truss elements (Elements 9) which have no flexural stiffness. The FE model was partitioned into 13812 elements, with the total number of 14585 nodes.

The relative sliding behavior between the unbonded tendons and surrounding concrete could be simulated by using options provided in MARC, namely, Links and Nodal ties. The truss nodes (with 3 translational degrees of freedom) for the tendons were defined as tied nodes, while the shell nodes at the same locations for the concrete cylinder were defined as retained nodes. There were two ways of tying between the tied nodes and the retained nodes: 1) except for the anchors, the tied nodes were constrained in the two transverse directions while the longitudinal degree of

freedom was free and 2) at the location of the anchors, the 3 degrees of freedom of the tied nodes were tied respectively to those of the retained nodes. In order to achieve the designed hoop and vertical compressive stresses in concrete cylinder, initial tensile stresses were applied on the tendons.
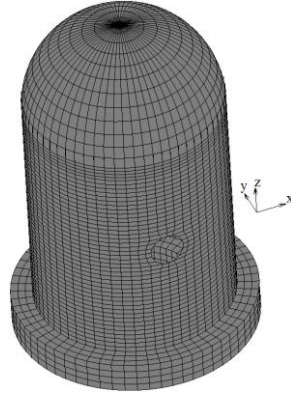

Fig. 2 3D FE model for the 1:10 scale UPCCV

Table 1 Scale factors for the 1:10 test model structure

Parameter	Symbol	Relationship	Scale factor (model: prototype)
Length	S_l	S_l	1:10
Mass density	S_ρ	S_ρ	1:1
Elastic modulus	S_e	S_e	1:1
Time	S_t	$S_l\sqrt{S_\rho/S_e}$	1:10
Frequency	S_f	$\sqrt{S_\rho/S_e}/S_l$	10:1
Acceleration	S_a	$S_e/(S_l \times S_\rho)$	10:1
Displacement	S_u	S_l	1:10
Stress	S_σ	S_e	1:1
Strain	S_ε	S_e	1:1
Force	S_F	$S_e \times S_l{}^2$	1:100

Table 2 Material properties used in the analysis

Material	Yong's modulus /GPa	Poisson's ratio	Yield strength /MPa	Mass density / (kg·m⁻³)
Concrete	35.5	0.2	—	2500
Tendons	195	0.3	1860	7850
Rebars	200		500	

3.2 Modelling of the material

Concrete in compression was treated as an elastic–plastic material using the Buyukozuturk yield criterion (Buyukozturk 1977) with an associated flow rule and a combined hardening rule. To define the uniaxial stress-strain relationship the equations suggested by Guo and Zhang (1982) was used

$$\frac{\sigma}{f_c} = \begin{cases} a \cdot \dfrac{\varepsilon}{\varepsilon_c} + (3 - 2a)\left(\dfrac{\varepsilon}{\varepsilon_c}\right)^2 + (a - 2)\left(\dfrac{\varepsilon}{\varepsilon_c}\right)^3, & 0 \le \varepsilon \le \varepsilon_c \\[2em] \dfrac{\dfrac{\varepsilon}{\varepsilon_c}}{b\left(\dfrac{\varepsilon}{\varepsilon_c} - 1\right)^2 + \dfrac{\varepsilon}{\varepsilon_c}}, & \varepsilon_c < \varepsilon \le \varepsilon_u \end{cases} \tag{1}$$

in which, σ is the compressive stress, ε is the compressive strain, f_c is the compressive strength which equals to 0.76 f_{cu}, ε_c is the peak strain and is taken as 0.002, ε_u is the crushing strain and is taken as 0.0033, a is the ascending branch parameter and is taken as 1.75, and b is the descending branch parameter which is taken as 2.59.

The smeared crack approach was adopted to simulate the tensile behavior of cracked concrete. It is assumed that the concrete behave as a linear elastic material and when the first principal stress reaches the tensile strength of the concrete (f_t = 4.2 MPa) cracks will develop in a direction normal to the principal stress.

For the steel materials (rebars, and tendons), the elasto-plastic theory based on von Mises yield criterion was adopted to represent the non-linear behavior.

The material properties of the concrete and the steel used in the analysis of the 1:10 UPCCV model are presented in Table 2.

3.3 Input of the earthquake response analysis

Three ground motion accelerograms were used in the analysis: 1) an artificial earthquake wave with the PGA of 0.3g (294 gal), which was also used as the ground excitation in the pseduo-dynamic test; 2) E-W component of the 11 March 2011 Japan earthquake recorded at the MYG003 station with the PGA of 781 gal (Kyoshin 2011a); and 3) E-W component of the 11 March 2011 Japan earthquake recorded at the MYG013 station with the PGA of 982 gal (Kyoshin 2011b). The design SSE has a maximum horizontal acceleration of 0.2g (196 gal). Thus, the PGA of the three ground motions in this investigation are 1.5, 4.0 and 5.0 times those of SSE respectively.

The acceleration time histories and acceleration response spectrums of the three earthquakes for the prototype are shown in Fig. 3, Figs. 4 and Fig. 5. It should be noted that for the last two records, the total duration time are 300s. However, the present study focused on the intense phase of 120s (ranging from 30s~150s). In addition, for the pseduo-dynamic test and the dynamic analysis of the 1:10 test model structure, these three records were scaled both in time and amplitude for similitude requirements (see Table 1).

There were five nonlinear time history analysis cases: Case 1 was used to validate the FE model by comparing the numerical results with the experimental response obtained from the
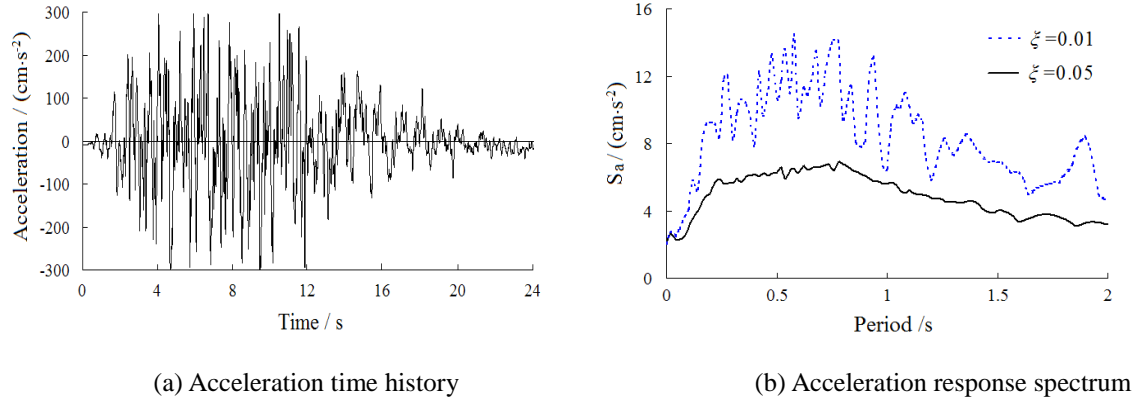
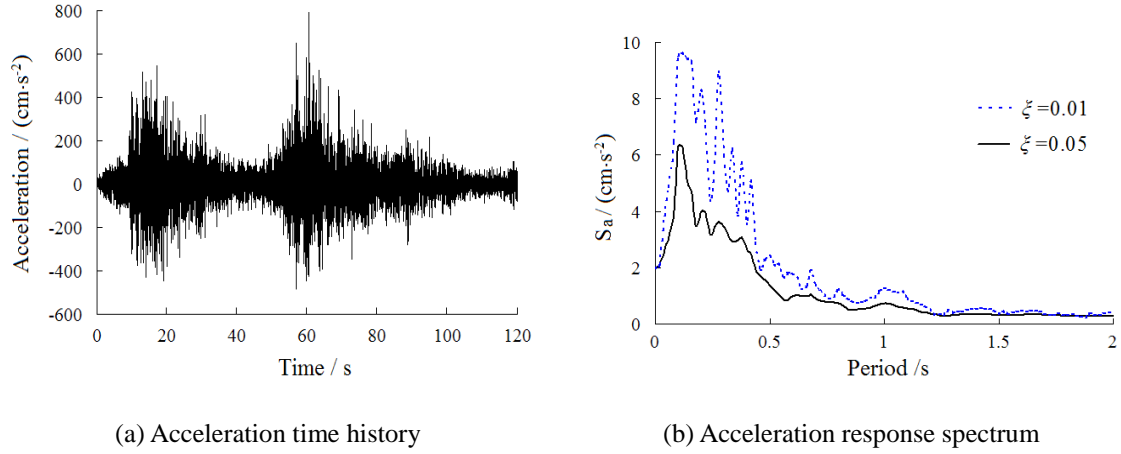*An Duan, Zuo-zhou Zhao, Ju Chen, Jia-ru Qian and Wei-liang Jin*

(a) Acceleration time history (b) Acceleration response spectrum

Fig. 3 Artificial earthquake

(a) Acceleration time history (b) Acceleration response spectrum

Fig. 4 Ground motion recorded at MYG003 station during the Japan's March 11, 2011 earthquake

(a) Acceleration time history (b) Acceleration response spectrum
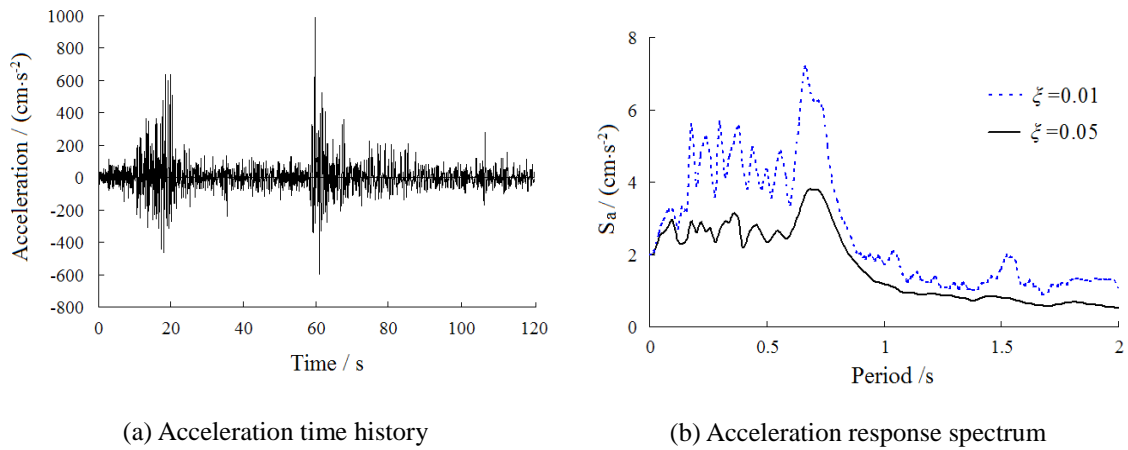
Fig. 5 Ground motion recorded at MYG013 station during the Japan's March 11, 2011 earthquake

Table 3 Main characteristics of the five time history analysis cases

Analysis case	Input wave	PGA/gal	Time duration/s	Input direction
1	Artificial wave	2940	2.4	*y* - axis
2	MYG003	7810		*y* - axis
3	MYG003		12	*x* - axis
4	MYG013	9820		*y* - axis
5	MYG013			*x-* - axis

pseduo-dynamic test. Case 2 to Case 5 were used to predict the response of the advanced UPCCV under Japan's March 11, 2011 earthquake. The main characteristics of the five analysis cases are listed in Table 3. Take Case 3 for instance, the E-W component of the 11 March 2011 Japan earthquake recorded at the MYG003 station was used as the input wave, the time duration was scaled to 12s and the PGA scaled to 7810 gal, and 0°- 180° (x-axis) was chosen as the direction of the excitation.

Rayleigh damping was assumed with a specified damping ratio (ξ) of 0.05 at both the first and second vibration modes of the 1:10 test model. Houbolt method (MSC 2007a) was used to integrate the equations of motion to obtain the dynamic response of the structural system. The nonlinear algebraic equations were solved iteratively by using Modified Newton-Raphson method (Ben-Israel 1966). The time interval of the artificial wave and the ground motions recorded at MYG003 (or MYG013) station are 0.005s and 0.01s respectively. Hence, a time step of 0.0005 was used in Case 1, and 0.001s in other dynamic analysis cases. The chosen time steps didn't exceed 10 percent of the period of the highest frequency of interest and were considered to be adequate for the dynamic analysis.

4. Analysis results and discussions

4.1 Validation of the FE model

Periods, frequencies and directions of the first six modes estimated from the analyses for the 1:10 scale UPCCV structure are given in Table 4. The frequencies in the direction of y-axis and x-axis for the prototype are 4.343 Hz and 4.377 Hz respectively (Qian *et al*. 2007). Hence, the relationship between the frequencies of the FE model and those of the prototype are in accord with the similitude laws.

As stated before, a pseudo-dynamic test of a 1:10 scale UPCCV structure has been carried out using the artificial wave (Fig. 3) with the PGA of 2940 gal as the ground motion. 90°-270° (y-axis) was chosen to be the direction of the excitation. Fig. 6 gives the displacement time history obtained from the pseudo-dynamic test and from Analysis Case 1. The displacement in the figure is the horizontal displacement on the top of the cylinder (at the elevation of 4800 mm) relative to the bottom of the cylinder. As can be seen, the calculated displacement time history showed good agreement with the experimental result, indicating that the analytical model in this study was reasonable and has the ability to predict the earthquake response of the UPCCV. Nevertheless, the peak values predicted by the analysis were about 15 percent lower than those obtained from the test. The occurrence of the deviance was mainly due to the following reasons: 1) there existed some construction geometry errors during the building of the test model, and 2) the properties of the actual concrete may differ a little from those used in the analysis.

An Duan, Zuo-zhou Zhao, Ju Chen, Jia-ru Qian and Wei-liang Jin

Table 4 First six modes

Mode	1st	2nd	3rd	4th	5th	6th
Period /s	0.0233	0.0229	0.0183	0.0167	0.0164	0.0149
Frequency/Hz	42.93	43.74	54.62	59.76	61.03	67.30
Direction	*y*	*x*	Torsion	Torsion	Torsion	Torsion

Table 5 Peak values of displacement and base shear force

Analysis Case	Input motion	Direction	Displacement/mm		Base shear force/ kN	
			Maximum	Minimum	Maximum	Minimum
Case 2	MYG003	*y*	1.56	-1.82	3500.4	-2650.4
Case 3		*x*	1.44	-1.93	3860.1	-2843.3
Case 4	MYG013	*y*	1.57	-1.94	4744.5	-2555.4
Case 5		*x*	1.46	-1.99	5017.3	-2546.6
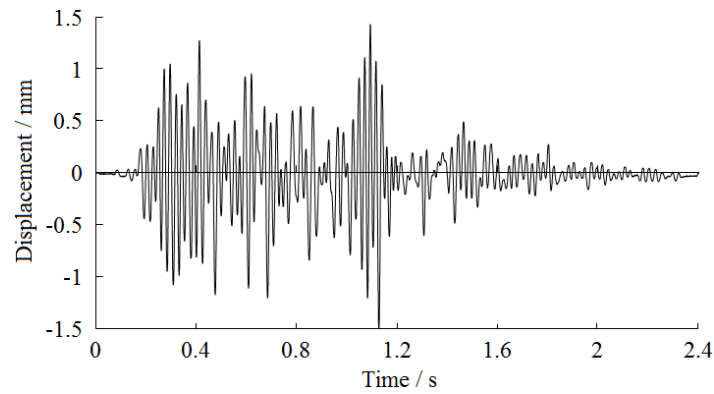
(a) Test results
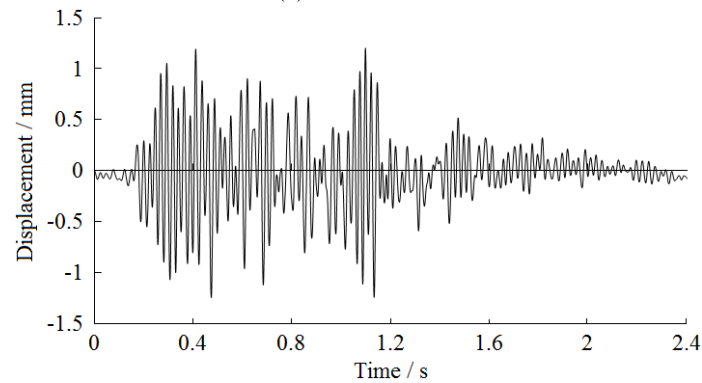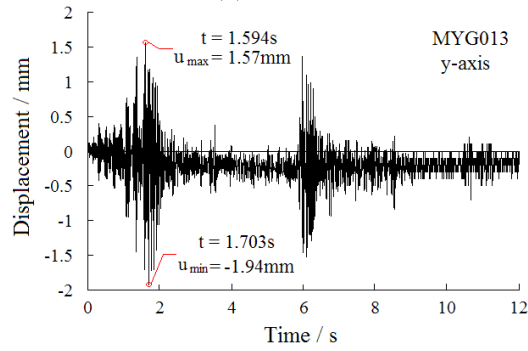

(b) Analysis results

Fig. 6 Displacement time history of a 1:10 scale UPCCV model under the artificial earthquake excitation (with the PGA of 2940 gal)
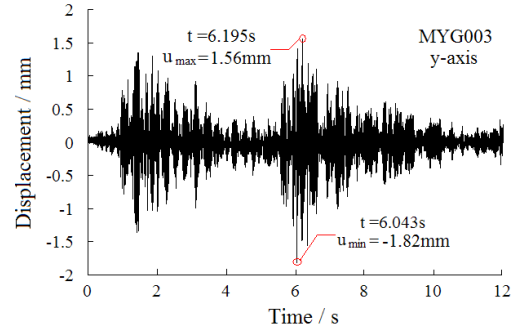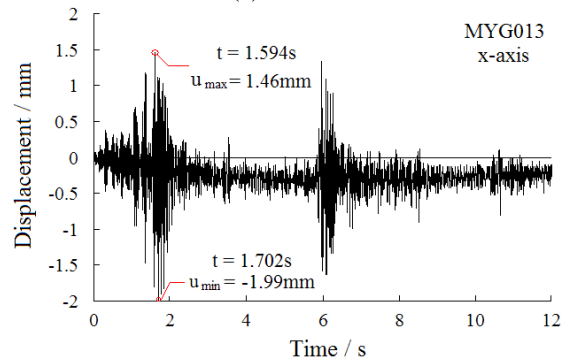
(a) Case 2
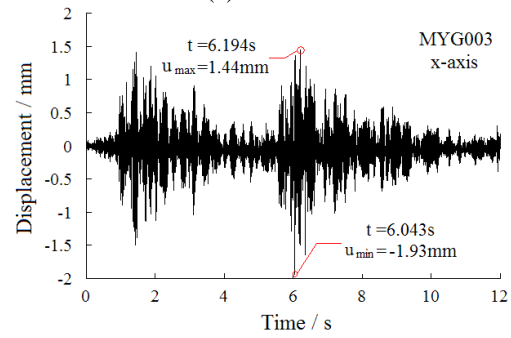
(b) Case 3

(c) Case 4

(d) Case 5

Fig. 7 Displacement time histories predicted by Case 2 to Case 5

4.2 Simulation results of case 2 to case 5

4.2.1 Displacements and base shear forces
    Fig. 7 presents the displacement (as defined in 4.1) time histories predicted by Case 2 to Case 5. The input ground record and the direction of the excitation are given on the upper right corner of each graph. Examination of Figs. 7(a) and (b) shows that the response of the 1:10 scale UPCCV model structure was elastic throughout the duration of the input of ground motion MYG003 and sustained no permanent displacement at the end of the record. However, when under MYG013 excitation, the UPCCV model structure showed inelastic deformation that caused some residual displacement. It should be noticed that according to the similitude law, the displacement response of the prototype should be ten times that of the 1:10 model structure.
    The peak values of the base shear force (BSF) of the 1:10 scale UPCCV structure during the four earthquake excitations are listed in Table 5. When the directions of the excitation were in y-axis, the maximum calculated BSFs were 3500 kN and 4745 kN for the MYG003 and MYG013 earthquakes, while the maximum BSF calculated using the artificial wave (Case 1) was 2082 kN.

4.2.2 Strains and stresses
    When subjected to the earthquake excitation, failure was more likely to occur in the cylinder than in the dome or the basement, thus emphasis of this research was placed on the behaviour of the cylinder. For brevity, only the results of the cylinder predicted in Case 4 are displayed. According to the similitude law (Table 1), the strain and stress would be 1:1 for the 1:10 model structure and the prototype.

4.2.2.1 Concrete
    It is noted that the maximum absolute value of the displacement and the maximum strains occur at the same time. Thus, the vertical strain distribution in the inner concrete layer of the cylinder at $t = 1.703$s (when the minimum displacement is reached) for Case 4 is shown in Fig. 8 (a). In general, the strains are within elastic limit. The lower parts of the cylinder on the 270° side were in tension, and the largest tensile vertical strain (261.5×10^{-6}) appeared at the elevation of 330 mm at 270° azimuth (Position 1). Concrete cracks on inner surface with a crack depth of 40% wall thickness occurred near the bottom of the cylinder. Fig. 8(b) displays the crack width distribution and highlights the area of the cracked concrete.
   The analysis showed that on the inner surface of the cylinder, flexural cracks developed near the bottom of the cylinder, while on the outer surface, cracks would appear near the device opening on the 90° side. The maximum tensile strain in the outer concrete layer occurred at 1.594s (when the maximum displacement was reached). Fig. 9 presents the strain contour at this moment.
    As can be observed, the largest tensile vertical strain (242.9×10^{-6}) of the outer layer is concentrated near the device opening (Position 2), while the largest compressive vertical strain (-378.6×10^{-6}) appears at the elevation of 330 mm at 270°azimuth (Position 1). The Cracks were noticed near the opening with a crack depth of 50% wall thickness from the outer surface. The main reasons for concrete cracking at this position are as follows. Firstly, the geometry discontinuity around the penetration caused stress concentration. Secondly, in the actual structure (i.e. prototype), a steel liner was used to strengthen the opening area, yet the FE model didn't take into account this liner since the 1:10 test structure model which we used for the simulation does not have this layer of steel liner in it for the sake of simplification of construction.
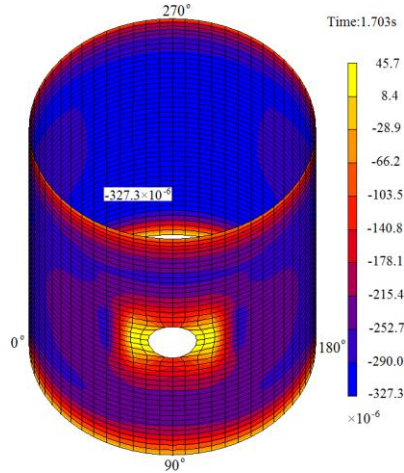   The vertical strain time histories at the two positions are given in Fig. 10. For position 2, it is
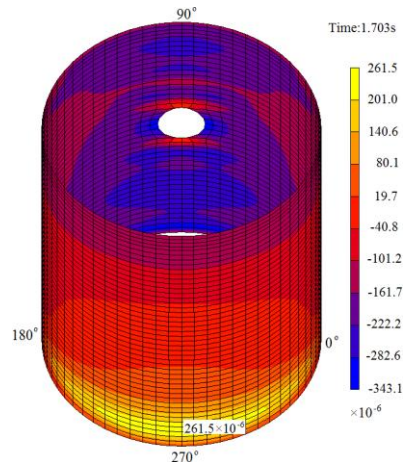
(a) Vertical strains
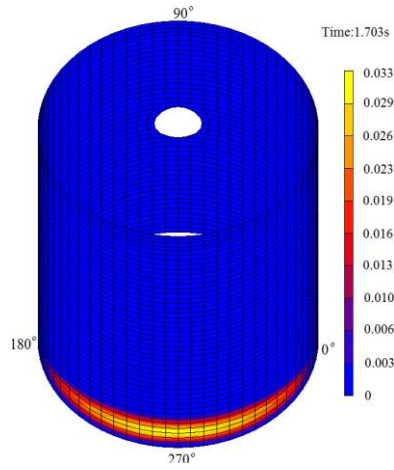
(b) Crack widths (Unit: mm)

(c) Hoop strains

Fig. 8 Strain and crack width distribution in the inner layer of the concrete cylinder at 1.703s for Case 4
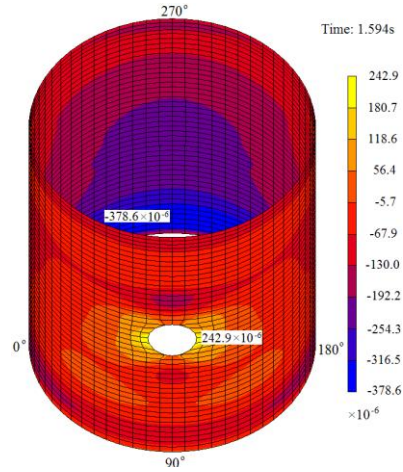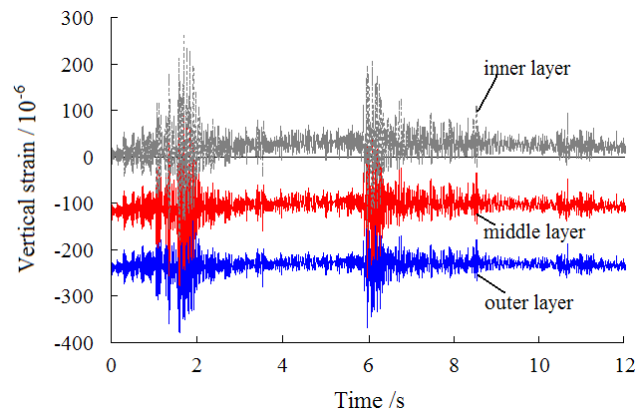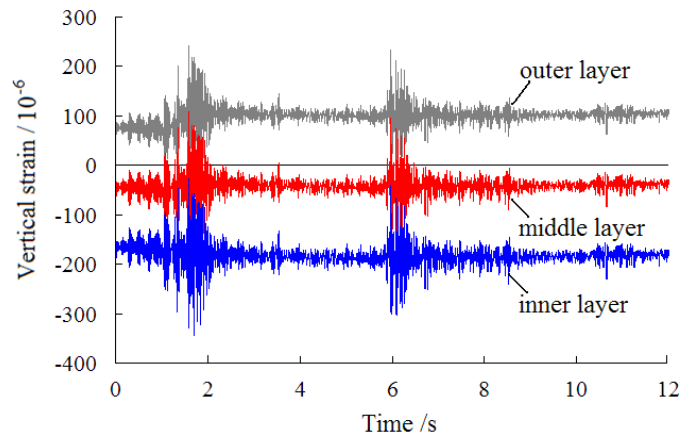
Fig. 9 Strain distribution in the outer layer of the concrete cylinder at 1.594s for Case 4


(a) Position 1

(b) Position 2

Fig. 10 Vertical strain time histories at the two positions for Case 4

observed that in the outer layer, progressive cracking near the device opening caused permanent residual strain at the end of the record. In the middle layer, the maximum strain was smaller than the cracking strain. Due to prestressing, the strain in the inner layer remained negative throughout the excitation. Position 1 showed the similar trend with Position 2 except that the cracks initiated from the inside surface. All the crack depths were within 50% of the wall thickness, and no through thickness cracking were observed during the excitation of MYG013.

Fig. 8(c) presents the hoop strain contour in the inner concrete layer of the cylinder at $t = 1.703$s. It is noticed that hoop compression due to prestressing is retained in almost the entire cylinder region. The maximum compressive hoop strain was at the elevation of 873 mm on the 270° side.

4.2.2.2 Rebar

Analysis results show that the rebar stresses are within elastic limit throughout the excitation of MYG013. The stresses of rebars in the cylinder at 1.703s for Case 4 are given in Fig. 11. The stress contours show that the vertical rebars are influenced by the deformation on the 90° and 270° sides which resist the overturning moment. As expected, the largest compressive and tensile stresses in the vertical rebars are concentrated at the bottom of 270° side and 90° side respectively. The stresses in the horizontal rebars of the cylinder are under compression except for the area around the opening and near the bottom of 270° side.
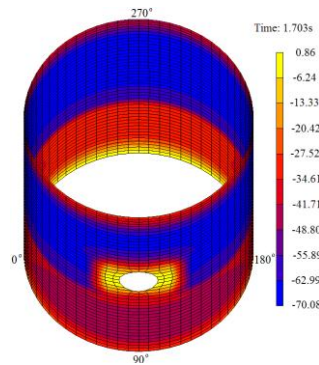
(b) Horizontal rebars

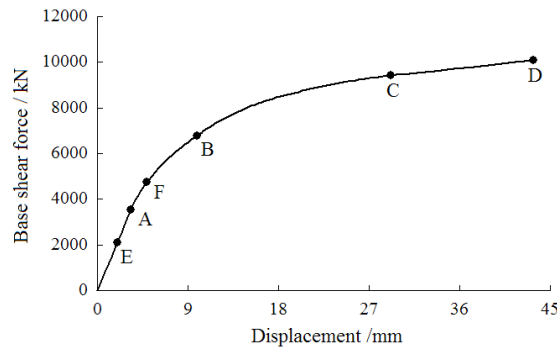Fig. 11 Stress distribution in the rebars of the cylinder at 1.703 s for Case 4 (unit: MPa)

Fig. 12 Base shear force –displacement predicted by the static analysis

4.3 Nonlinear static analysis

To seek the ultimate load carrying capacity of the UPCCV, a nonlinear static analysis of the 1:10 scale model structure was carried out. A monotonically increased lateral force was applied on the top of the cylinder, and the loading direction was in y-axis.

Fig. 12 presents the relation of BSF versus displacement predicted by the static analysis. The displacement in the figure is also the horizontal displacement on the top of the cylinder relative to the bottom of the cylinder. The characteristics of this curve and the main sequence of events during the lateral loading of the 1:10 scale UPCCV can be summarized as follows. The BSF-displacement curve is nearly linear up to BSF about 3540 kN (Point A), indicating the structure is in general within elastic stage, and no cracks are observed in the structure except around the device opening. Then, flexural cracks appear near the cylinder-base junction of the 90° side, and the structure begins to soften. At 6791 kN (Point B), the vertical rebar yielding initiated at the bottom of 90° side follows by cracked zone spreading to a larger region, and the force-displacement curve bends more sharply. At about 9428 kN (Point C), the vertical tendons at the azimuth of 90° begin to yield. At 10098 kN (Point D), the crushing strains in concrete are reached at the base of the cylinder within the range of 270° ± 40°. The BSFs at Point F and E are equal to the maximum BSFs during the excitations of MYG013 and the artificial wave (1.5 SSE) respectively.

There are two failure modes for the UPCCV: 1) tendon yielding; and 2) concrete crushing. Based on criterion 1, the ultimate lateral load resisting capacity of the 1:10 scale UPCCV is 9428 kN, 2.0 times the maximum BSF (4745 kN) during the MYG013 earthquake excitation (Case 4), and 4.5 times the maximum BSF (2082 kN) during the 1.5SSE excitation (Case 1). According to criterion 2, the ultimate lateral load capacity would be 10098 kN.

5. Conclusions

The main purpose of the present study is to evaluate the behaviour of the advanced UPCCV for one typical China nuclear power plant under Japan's March 11 earthquake. Five nonlinear time history analysis and a nonlinear static analysis of a 1:10 scale UPCCV structure have been carried out with MARC FE program. From the results of the analysis, the following statements can be concluded:

1) The calculated displacement time history predicted by Case 1 shows good agreement with the pseudo-dynamic test result, demonstrating that the analytical model in this study is reasonable and is capable of predicting the earthquake response of the UPCCV.

2) The 1:10 scale UPCCV model responded elastically throughout the duration of the input of ground motion MYG003.

3) When subjected to MYG013, the UPCCV model showed inelastic deformation that caused some residual displacement. The results of Case 4 show that on the inner surface of the cylinder, flexural cracks would develop near the bottom of the cylinder, while on the outer surface cracks would appear near the device opening on the 90° side. Besides, all the crack depths were within 50% of the wall thickness. The hoop compression in concrete due to prestressing was retained in almost the entire cylinder region. The stresses of the vertical and horizontal rebars were within elastic limit throughout the excitation of MYG013.

4) According to the tendon yielding failure criterion, the ultimate lateral load capacity of the

1:10 scale UPCCV is 9428 kN, 2.0 times the maximum BSF(4745 kN) during the MYG013 excitation, and 4.5 times the maximum BSF (2082 kN) during the 1.5SSE excitation.

Acknowledgements

References

Bash, S.M., Singh, R.K., Patnaik, R., Kushwaha, H.S. and Venkat Raj, V. (2003), "Predictions of ultimate load capacity for pre-stressed concrete containment vessel model with BARC finite element code ULCA", *Ann. Nucl. Energy*, **30**(4), 437-471.

Ben-Israel, A. (1966), "A newton-raphson method for the solution of systems of equations", *J. Math. Anal. Appl.*, **15**(2), 243-252.

Buyukozturk, O. (1977), "Nonlinear analysis of reinforced concrete structures", *Comput. Struct.*, **7**(1), 149-156.

Duan, A. and Qian, J.R. (2009), "Aseismic safety analysis of a containment vessel model for CNP1000 nuclear power plant", *Eng. Mech.*, **26**(4), 153-157(in Chinese).

Frano, R.L., Pugliese, G. and Forasassi, G. (2010), "Preliminary seismic analysis of an innovative near term reactor: Methodology and application", *Nucl. Eng. Des.*, **240**(6), 1671-1678.

Guo, Z.H. and Zhang, X.Q. (1982), "Experimental investigation of the complete stress-strain curve of concrete", *J. Build. Struct.*, **3**(1), 1-12 (in Chinese).

Hirama, T., Goto, M., Hasegawa, T., Kanechika, M., Kei, T., Mieda, T., Abe, H., Takiguchi, K. and Akiyama, H. (2005a), "Seismic proof test of a reinforced concrete containment vessel (RCCV), Part 1: Test model and pressure test", *Nucl. Eng. Des.*, **235**(13), 1335-1348.

Hirama, T., Goto, M., Shiba, K., Kobayashi, T., Tanaka, R., Tsurumaki, S., Takiguchi, K. and Akiyama, H. (2005b), "Seismic proof test of a reinforced concrete containment vessel (RCCV), Part 2: Results of shaking table test", *Nucl. Eng. Des.*, **235**(13), 1349-1371.

Harris, H.G. and Sabnis, G.M. (1999), *Structural Modelling and Experimental Techniques*, (2nd Edition), CRC Press, Boca Raton, FL, USA

Kobayashi, T., Yoshikawa, K., Takaoka, E., Nakazawa, M. and Shikama, Y. (2002), "Time history nonlinear earthquake response analysis considering materials and geometrical nonlinearity", *Nucl. Eng. Des.*, **212**(1-3), 145-154.

Kyoshin Net. (2011a), "MYG0031103111446[1]", http://www.k-net.bosai.go.jp/. [2011-5-10]

Kyoshin Net. (2011b), "MYG0131103111446[1]", http://www.k-net.bosai.go.jp/. [2011-5-10]

Lee, N.H. and Song, K.B. (1999), "Seismic capability evaluation of the prestressed reinforced concrete containment, Yonggwang nuclear power plant Units 5 and 6", *Nucl. Eng. Des.*, **192**(2-3),189-203.

Li, Y., Lu, X.Z., Guan, H. and Ye, L.P. (2011), "An improved tie force method for progressive collapse resistance design of reinforced concrete frame structures", *Eng. Struct.*, **33**(10), 2931-2942.

Lu, X.Z., Teng, J.G., Ye, L.P. and Jiang, J.J. (2007), "Intermediate crack debonding in FRP-strengthened RC beams: FE analysis and strength model", *J. Compos. Construct.*, **11**(2), 161-174.

Lu, X.Z., Ye, L.P., Ma, Y.H. and Tang, D.Y. (2012), "Lessons from the collapse of typical RC frames in Xuankou school during the Great Wenchuan Earthquake", *Adv. Struct. Eng.*, **15**(1), 139-153.

MSC. Software Corporation (2007a), "MSC.MARC 2007 (Volume A): Theory and user information".

MSC. Software Corporation (2007b), "MSC.MARC 2007 (Volume B): Element library".

Miao, Z.W., Ye L.P., Guan, H. and Lu, X.Z. (2011), "Evaluation of modal and traditional pushover analyses in frame-shear-wall structures", *Adv. Struct. Eng.*, **14**(5), 815-836.

Prinja, N.K., Shepherd, D. and Curley, J. (2005), "Simulating structural collapse of a PWR containment", *Nucl. Eng. Des.*, **235**(17-19), 2033-2043.

Qian, J.R., Zhao, Z.Z., Duan, A., Xia, Z.F. and Wang, M.D. (2007), "Pseudo-dynamic tests of a 1:10 model of pre-stressed concrete containment vessel for CNP1000 nuclear power plant", *China Civil Eng. J.*, **40**(6), 7-13 (in Chinese).

CC